

2009

The Effect of Dielectric Friction on the Rate of Charge Separation in Type I ZnSe/Cds Semiconductor Nanorods

Alexander N. Tarnovsky

Bowling Green State University - Main Campus, atarnov@bgsu.edu

Nishshanka N. Hewa-Kasakarage

Patrick Z. El-Khoury

Nickolas Schmall

Maria Kirsanova

See next page for additional authors

Follow this and additional works at: http://scholarworks.bgsu.edu/chem_pub

 Part of the [Chemistry Commons](#)

Repository Citation

Tarnovsky, Alexander N.; Hewa-Kasakarage, Nishshanka N.; El-Khoury, Patrick Z.; Schmall, Nickolas; Kirsanova, Maria; Nemchinov, Alexander; Bezryadin, Alexey; and Zamkov, Mikhail, "The Effect of Dielectric Friction on the Rate of Charge Separation in Type I ZnSe/Cds Semiconductor Nanorods" (2009). *Chemistry Faculty Publications*. Paper 34.

http://scholarworks.bgsu.edu/chem_pub/34

This Article is brought to you for free and open access by the Chemistry at ScholarWorks@BGSU. It has been accepted for inclusion in Chemistry Faculty Publications by an authorized administrator of ScholarWorks@BGSU.

Author(s)

Alexander N. Tarnovsky, Nishshanka N. Hewa-Kasakarage, Patrick Z. El-Khoury, Nickolas Schmall, Maria Kirsanova, Alexander Nemchinov, Alexey Bezryadin, and Mikhail Zamkov

The effect of dielectric friction on the rate of charge separation in type II ZnSe/CdS semiconductor nanorods

Nishshanka N. Hewa-Kasakarage,¹ Patrick Z. El-Khoury,² Nickolas Schmall,¹ Maria Kirsanova,¹ Alexander Nemchinov,¹ Alexander N. Tarnovsky,² Alexey Bezryadin,³ and Mikhail Zamkov^{1,a)}

¹*Department of Physics and Astronomy and The Center for Photochemical Sciences, Bowling Green State University, Bowling Green, Ohio 43403, USA*

²*Department of Chemistry and The Center for Photochemical Sciences, Bowling Green State University, Bowling Green, Ohio 43403, USA*

³*Department of Physics, University of Illinois Urbana-Champaign, 1110 West Green St., Urbana, Illinois 61801-3080, USA*

(Received 6 February 2009; accepted 12 March 2009; published online 3 April 2009)

The effect of dielectric friction on the rate of charge separation in type II ZnSe/CdS semiconductor nanorods has been investigated using picosecond transient absorption spectroscopy. The spatial separation of an excited electron-hole pair was estimated from the redshift in band edge absorption corresponding to the decrease in the exciton binding energy. The present study identifies a considerable effect of the solvent polarity on the rate of charge separation in semiconductor heterostructures, which should be taken into account when selecting nanorod caging media, such as solvents or polymer matrices. © 2009 American Institute of Physics. [DOI: 10.1063/1.3114464]

The spatial separation of photogenerated charges is a key requirement for an efficient generation of chemical energy from light in a variety of optoelectronic devices. For semiconductor nanocrystals (NCs), such charge separation is achieved via a two-component heterojunction with a type II or staggered energy alignment at the interface for which both the valence and conduction bands of one component lie lower in energy than the corresponding bands of the other component. The inorganic coupling of materials in such heterostructure realized either in a symmetric core/shell,¹⁻⁵ or asymmetric dot-rod,⁶ or branched⁷ assembly ensures an efficient and rapid separation of excited carriers, which, combined with a low-cost organometallic synthesis should stimulate the incorporation of these materials into emerging photovoltaic and photocatalytic technologies.

To date several combinations of II-VI semiconductors, including CdS/CdSe,^{8,9} CdSe/CdTe,⁶ and ZnSe/CdS (Refs. 10 and 11) have been considered to enhance the photoinduced charge separation in heterostructured NCs. Thus far, the most encouraging characteristics both in terms of an electron-hole separation¹² and low spatial overlap of the corresponding wave functions were demonstrated for ZnSe-seeded CdS nanorods (NRs). In addition, unlike CdSe/CdTe or CdSe/CdS-based heterostructures, ZnSe/CdS NRs also exhibit strong fluorescence associated with type II relaxation of carriers across the ZnSe/CdS junction, with lifetimes in the order of 200–300 ns,^{10,11} which is sufficient for excited carriers to be transferred to an electrode or metal nanoparticle during a photovoltaics and photocatalytic conversion.

The amount of time required for a complete separation of charges plays an important role in many optoelectronic applications of type II heterostructures, including electroabsorption modulators¹³ where the rate of the device operation depends on the speed with which charges are brought into a separated state or multiple exciton generation-based photo-

voltaic devices,¹⁴ where electron-hole separation should be fast enough to precede exciton-exciton annihilation.¹⁵ For structures with a spatially asymmetric charge distribution, such as ZnSe/CdS NRs, the rate of charge separation depends on the surrounding media, though a phenomenon known as dielectric friction (DF), which results from the work necessary to orientate external dipoles in response to the motion of charges within the NR. Since the orientational response of the medium is not instantaneous, it affects the charge separation time. Previous works have identified a central role of DF in ionic mobility and dipolar orientational relaxation¹⁶ and later on in charge transfer dynamics¹⁷ and dipole isomerizations;¹⁸ on the other hand, its effect on carrier mobility in colloidal NCs is majorly unknown.

Here we investigate the effect of DF on the dynamics of charge separation in ZnSe/CdS NRs by measuring the bleach recovery times of band edge excitons. The dielectric media were introduced by dispersing NRs in solvents with different polarities. Temporal evolution of the excited state population was measured using transient absorption (TA) technique. Present measurements confirm an apparent negative correlation between the solvent polarity and the charge separation rate, which is explained as due to DF effect on carrier mobility.

Figure 1 shows a type II alignment of band edges in ZnSe/CdS NRs, which favors electrons localization along CdS branches and holes within ZnSe NCs. Such spatially separated arrangement of charges has been experimentally confirmed for ZnSe/CdS NRs using scanning tunneling microscope (Ref. 12) and TA (Ref. 11) techniques as well as through the observation of the quantum-confined Stark effect in NRs, in which the axes are parallel to the direction of the electric field.¹¹ In the present study, changes in the degree of charge separation along the rod axis were monitored by measuring the corresponding change in the energy of $1S_e(\text{CdS}) - 1S_h(\text{ZnSe})$ transition through an empirical equation¹⁹ that relates the position of the absorption peak to the effective electron-hole separation, l_{eff} . Model calculations based on

^{a)}Electronic mail: zamkovm@bgsu.edu.

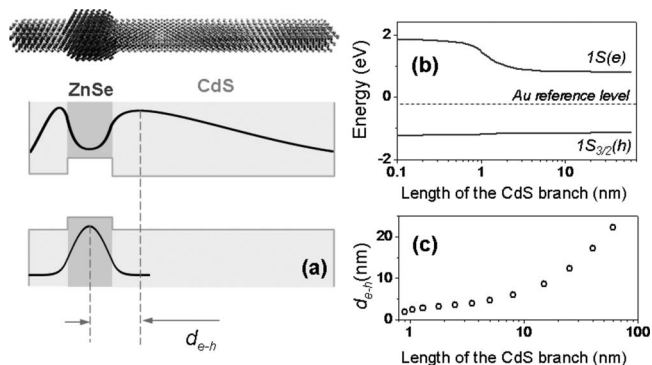


FIG. 1. (a) Relative positions of the conduction and valence band edges in a ZnSe/CdS heterostructure, along with corresponding electron ($1S_e$) and hole ($1S_{3/2h}$) excited state wave functions. (b) The dependence of zero-angular momentum state energies on the length of CdS branch. (c) Expected spatial separation of an electron-hole pair vs the length of CdS branch.

known solutions to envelope-function Schrödinger equation for noninteracting carriers²⁰ were also employed to estimate the effect of the CdS length on the maximum value of l_{eff} and the corresponding recombination energy. Results of these calculations,¹⁹ shown in Figs. 1(b) and 1(c), provided guidance in selecting a suitable range of NR lengths that ensures large values of l_{eff} , and simultaneously allows for a sufficient separation-induced changes in $1S_e(\text{CdS})-1S_h(\text{ZnSe})$ transition energies that can be discriminated via TA measurements. Based on this analysis we have chosen 90-nm-long NRs for which the value of l_{eff} is approximately 20 nm [Fig. 1(c)].

Colloidal ZnSe/CdS NRs were fabricated via organometallic routes, according to a previously developed three-step procedure that involves synthesis of ZnSe NCs, deposition of a thin CdS shell,⁵ and subsequent growth of CdS extensions.¹⁹ Typical transmission electron microscope (TEM) images of as-prepared NRs are shown in Figs. 2(a) and 2(b). The difference in growth rates of CdS in each of the two directions results in the off-center position of ZnSe/CdS seeds in the final structure, as seen in Fig. 2(b). After precipitating from the growth solution, NRs were thoroughly cleaned and redispersed in several solvents with different polarities. In this work we have chosen CCl_4 ($\epsilon=2.2$), CHCl_3 ($\epsilon=4.8$), and dichloromethane (DCM, $\epsilon=9.1$) solvents that allowed for NR concentrations to be within the linear Beer-Lambert regime.

Steady-state absorption and emission spectra of ZnSe/CdS NRs suspended in the three solvents are shown in Fig. 2(c). Previous reports^{10,11} have identified the origin of the main absorption edge at 500 nm as $1S_e-1S_{3/2h}$ transition in the CdS portion of the rod, while the low-energy tail (550–620 nm) was assigned to the $1S_e(\text{CdS})-1S_h(\text{ZnSe})$ transition in the interfacial area. Comparison of the absorption spectra in Fig. 2(c) reveals a negligible effect of the solvent polarity on the position of the main absorption edge. Indeed, spectral differences between CCl_4 - and CHCl_3 -suspended NRs are minimal, while the increased low-energy absorption of DCM-suspended NRs is likely the result of the inferior solubility of NR in DCM, which was consistent with a lower emission quantum yield for that case. Similarly, comparison of NR emission spectra also did not show significant solvent effects. As seen in Fig. 2(c), both the position and the width of FL peaks arising from $1S_e(\text{CdS})-1S_h(\text{ZnSe})$ carrier recombination remain the same in all three solvents, indicating

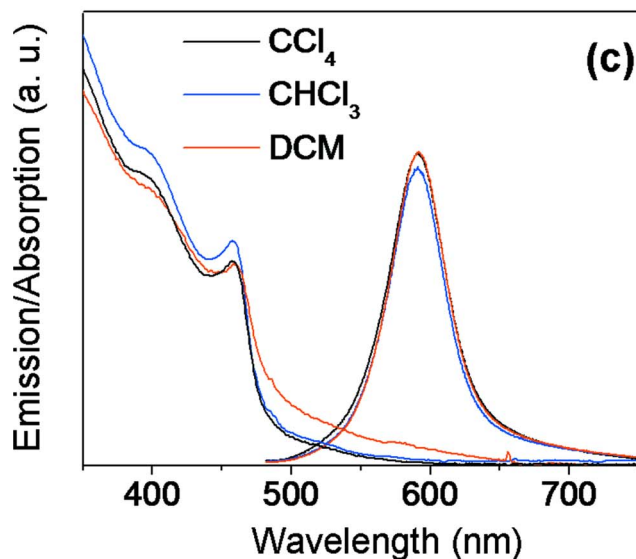
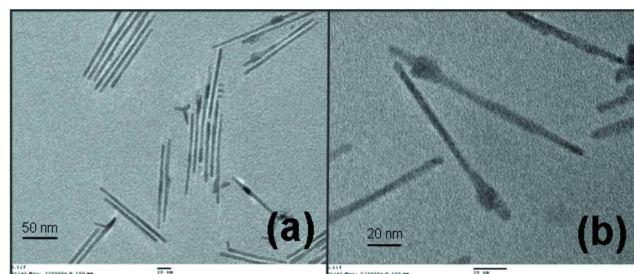


FIG. 2. (Color online) [(a) and (b)] TEM images of ZnSe/CdS NRs. (c) Steady-state absorption and emission spectra of ZnSe/CdS NRs in CCl_4 , CHCl_3 , and DCM (CH_2Cl_2) solvents.

that energies of $1S_e(\text{CdS})$ and $1S_h(\text{ZnSe})$ states are not screened by the surrounding dielectric media.

The dynamics of charges separation in ZnSe/CdS NRs was investigated using picosecond TA spectroscopy. The experimental setup was based on the Ti:sapphire laser operating at a repetition rate of 1 kHz, which output was split into two components: one was directed through the TOPAS OPA to produce excitation pulses at 420 nm, and the second one was focused onto a CaF_2 plate to generate a white-light-continuum for broadband probe pulses (see supporting information).¹⁹ All TA data were corrected for the group velocity dispersion of the white-light continuum by using the nonresonant signals of pure solvents. The incident excitation pulse was attenuated before the sample position to minimize the solvent contribution due to nonlinear pump absorption.

Figure 3(a) shows a typical TA spectrum of CCl_4 -suspended NRs that contains two primary intervals of bleaching ($\Delta\alpha$ minima) at 455 and 540 nm, corresponding to $1S_e-1S_{3/2h}$ transitions in the CdS branch and ZnSe/CdS heterojunction, respectively. By using 1 ps of minimal delay between excitation and probe pulses we ensure that most carriers occupying high-energy states ($nS, nP, \dots, n > 1$) relax to band edges,^{21,22} such that the primary contribution to the bleaching signal comes from $1S_e, h$ states. The recovery of 540 nm bleach for ZnSe/CdS NRs suspended in CCl_4 , CHCl_3 , and DCM solvents are shown in Fig. 3(d). In contrast to the adiabatic recovery of the 455 nm signal from $1S_e1S_h(\text{CdS})$ excitons, the spectral position of the 540 nm bleach, corresponding to the interfacial relaxation, gradually

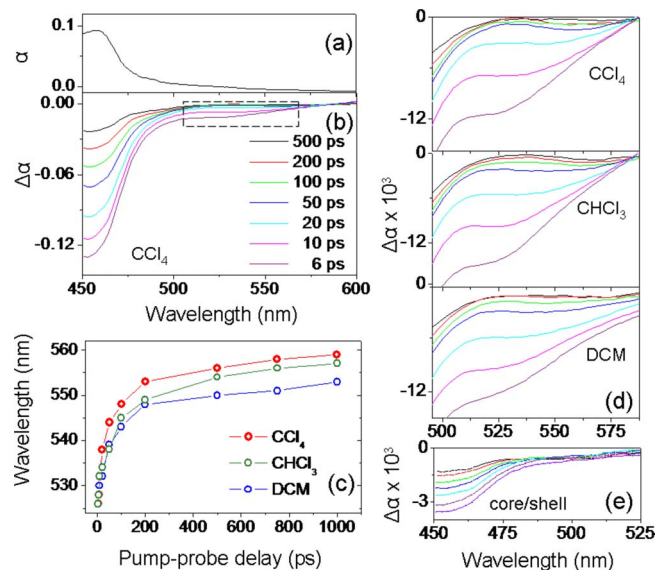


FIG. 3. (Color online) (a) Steady-state absorption α of ZnSe/CdS NRs dispersed in CCl_4 . (b) Absorbance changes $\Delta\alpha$ in CCl_4 -suspended NRs excited with 420 nm monochromatic light. The area highlighted with a dashed rectangle is shown in more detail in (d) for CCl_4 -, CHCl_3 -, and DCM-suspended NRs. (c) Temporal evolution of the bleach shift for all three solvents. (e) $\Delta\alpha$ of core/shell ZnSe/CdS NCs suspended in nonpolar hexane.

redshifts from 525 to 550 nm over the period of 200 ps. This process is sufficiently slower than the decay of high-energy carriers to the bottom of the band, indicating that the change in the energy of the $\Delta\alpha$ minimum cannot be associated with either $2S_{3/2}(h)-1S_{3/2}(h)$ or $1P(e)-1S(e)$ carrier relaxation pathways. Instead, the observed shift in the 540 nm bleach can be linked to the decrease in the spatial confinement of electronic wave functions associated with a charge separated state, as predicted by model calculations shown in Fig. 1(b). This explanation is also consistent with the absence of the spectral shift in the $\Delta\alpha$ minimum for core/shell ZnSe/CdS NCs, where electrons are restricted to a small volume of CdS shell [Fig. 3(e)].

Temporal changes in the spectral position of $\Delta\alpha$ minima for the three solvents are compared in Fig. 3(c). The fastest shift was observed for NRs suspended in nonpolar CCl_4 (red curve), while the most polar, DCM-suspended NR (blue curve) produced the slowest change in the $\Delta\alpha$ position. Overall, during the 1 ns scan, $\Delta\alpha$ minima for NR in CCl_4 , CHCl_3 , and DCM redshifted by 50, 60, and 70 nm, respectively, which confirms a sizable effect of the solvent polarity on the interfacial carrier relaxation rate. In particular, for NRs suspended in nonpolar CCl_4 , the energy of the $1S$ exciton approaches the steady-state limit of the absorption energy (2.1 eV), which indicates a near complete electron-hole separation along the NR axis. In DCM-suspended NR, however, even after 1 ns, exciton energy still remains 0.4 eV above the corresponding band gap value, which, according to Fig. 1(b), corresponds to an effective electron-hole separation of 2 nm. This is significantly smaller than the 18 nm delocalization of electronic wave functions along the 70 nm CdS branch expected from model calculations¹⁹ [see Fig. 1(c)].

The effect of solvent polarity on charge separation rate in NRs can be understood in term of the energy exchange with the surrounding dielectric media (DF) that impedes the delocalization of electrons into CdS. Indeed, polar solvent molecules require more energy to orient along the direction

of the electric field, causing some of the energy absorbed by NRs to be dissipated into the surrounding dielectric media. Such energy exchange is consistent with the observation of nearly identical rates in CCl_4 and DCM for the initial increase in the $\Delta\alpha$ position from 525 to 540 nm, since the corresponding spatial shift in the electronic wave function for this case is expected to be less than 1 nm. On the other hand, when the $\Delta\alpha$ minimum redshifts from 540 to 550 nm, an electron penetration into CdS increases to 10 nm thus causing more energy to be dissipated into the solvent, which is manifested by the difference of charge separation rates for this interval [Fig. 3(c)]. Based on the proportional delay of charge separation rates in CCl_4 , CHCl_3 , and DCM-suspended NRs, as well as the positive correlation of the friction effect with the expected delocalization of electrons along CdS branch, we attribute observed changes in bleach recovery to the solvent DF.

In conclusion, we show that the solvent polarity has a considerable effect on the rate of charge separation in semiconductor heterostructures and should be considered in the development of NR caging materials, including polymer matrices, solvents, and substrates.

We gratefully acknowledge Bowling Green State University for financial support (Grant Nos. SF07, RIC2008, and RCE2008).

- ¹S. Kim, B. Fisher, H. J. Eisler, and M. Bawendi, *J. Am. Chem. Soc.* **125**, 11466 (2003).
- ²K. Yu, B. Zaman, S. Romanova, D. Wang, and J. Ripmeester, *Small* **1**, 332 (2005).
- ³M. Danek, K. F. Jensen, C. B. Murray, and M. G. Bawendi, *Chem. Mater.* **8**, 173 (1996).
- ⁴A. Pandey and P. Guyot-Sionnest, *J. Chem. Phys.* **127**, 104710 (2007).
- ⁵A. Nemchinov, M. Kirsanova, N. N. Hewa-Kasakarage, and M. Zamkov, *J. Phys. Chem. C* **112**, 9301 (2008).
- ⁶S. Kudera, L. Carbone, M. F. Casula, R. Cingolani, A. Falqui, E. Snoeck, W. J. Parak, and L. Manna, *Nano Lett.* **5**, 445 (2005).
- ⁷D. J. Milliron, S. M. Hughes, Y. Cui, L. Manna, J. Li, L. Wang, and A. P. Alivisatos, *Nature (London)* **430**, 190 (2004).
- ⁸D. V. Talapin, R. Koeppel, S. Gotzinger, A. Kornowski, J. M. Lupton, A. L. Rogach, O. Benson, J. Feldmann, and H. Weller, *Nano Lett.* **3**, 1677 (2003).
- ⁹J. Müller, J. M. Lupton, A. L. Rogach, J. Feldmann, D. V. Talapin, and H. Weller, *Phys. Rev. Lett.* **93**, 167402 (2004).
- ¹⁰D. Dorfs, A. Salant, I. Popov, and U. Banin, *Small* **4**, 1319 (2008).
- ¹¹N. N. Hewa-Kasakarage, M. Kirsanova, A. Nemchinov, N. Schmall, P. Z. El-Khoury, A. N. Tarnovsky, and M. Zamkov, *J. Am. Chem. Soc.* **131**, 1328 (2009).
- ¹²D. Steiner, D. Dorfs, U. Banin, F. D. Sala, L. Manna, and O. Millo, *Nano Lett.* **8**, 2954 (2008).
- ¹³J. S. Park, R. P. G. Karunasiri, and K. L. Wang, *J. Vac. Sci. Technol. B* **8**, 217 (1990).
- ¹⁴R. D. Schaller, V. M. Agranovich, and V. I. Klimov, *Nat. Phys.* **1**, 189 (2005).
- ¹⁵V. I. Klimov, *Annu. Rev. Phys. Chem.* **58**, 635 (2007).
- ¹⁶P. G. Wolynes, *Annu. Rev. Phys. Chem.* **31**, 345 (1980).
- ¹⁷R. A. Marcus and N. Sutin, *Biochim. Biophys. Acta* **811**, 265 (1985); M. D. Newton and N. Sutin, *Annu. Rev. Phys. Chem.* **35**, 437 (1984).
- ¹⁸G. V. D. Zwant and J. T. Hynes, *J. Phys. Chem.* **89**, 4182 (1985).
- ¹⁹See EPAPS Document No. E-APPLAB-94-048914 for details of synthesis and model calculations. For more information on EPAPS, see <http://www.aip.org/pubservs/epaps.html>.
- ²⁰A. Piryatinski, S. A. Ivanov, S. Tretiak, and I. V. Klimov, *Nano Lett.* **7**, 108 (2007).
- ²¹J. Puls, V. Jungnickel, F. Henneberger, and A. Chulzgen, *J. Cryst. Growth* **138**, 1004 (1994).
- ²²T. W. Roberti, N. J. Cherepy, and J. Z. Zhang, *J. Chem. Phys.* **108**, 2143 (1998).